

See discussions, stats, and author profiles for this publication at: <https://www.researchgate.net/publication/257362576>

# Organic–inorganic composite polymer electrolyte based on PEO–LiClO<sub>4</sub> and nano–Al<sub>2</sub>O<sub>3</sub> filler for lithium polymer...

Article in *Journal of Alloys and Compounds* · October 2013

DOI: 10.1016/j.jallcom.2013.04.054

CITATIONS

24

READS

78

4 authors, including:



**Emad Masoud**

Benha University

12 PUBLICATIONS 58 CITATIONS

[SEE PROFILE](#)



**W.A. Bayoumy**

Benha University

24 PUBLICATIONS 225 CITATIONS

[SEE PROFILE](#)



**Mahmoud Mousa**

Benha University

78 PUBLICATIONS 536 CITATIONS

[SEE PROFILE](#)



# Organic–inorganic composite polymer electrolyte based on PEO–LiClO<sub>4</sub> and nano-Al<sub>2</sub>O<sub>3</sub> filler for lithium polymer batteries: Dielectric and transport properties



Emad M. Masoud\*, A.-A. El-Bellihi, W.A. Bayoumy, M.A. Mousa

Chemistry Department, Faculty of Science, Benha University, 13518 Benha, Egypt

## ARTICLE INFO

### Article history:

Received 22 January 2013

Received in revised form 14 March 2013

Accepted 9 April 2013

Available online 20 April 2013

### Keywords:

PEO-based polymer electrolyte

Ionic conductivity

Nano-composites

## ABSTRACT

Nano-Al<sub>2</sub>O<sub>3</sub> with an average size of 42 nm was prepared by pyrolysis method. PEO–LiClO<sub>4</sub> based composite polymer electrolyte was prepared using solution cast technique. The samples were characterized by X-ray diffraction (XRD), differential scanning calorimetry (DSC) and infra red (FT-IR) techniques. Effect of nano-Al<sub>2</sub>O<sub>3</sub> ceramic filler concentration on the composite structure and its electrical properties (DC-conductivity, AC-conductivity, dielectric constant, dielectric loss and impedance) at a frequency and temperature ranges of 0–10<sup>5</sup> Hz and 293–323 K, respectively was studied. Melting temperature (*T<sub>m</sub>*) of PEO decreased with addition of both LiClO<sub>4</sub> salt and nano-Al<sub>2</sub>O<sub>3</sub> filler due to increasing the amorphous state of polymer. All composite samples showed an ionic conductivity with the highest value for the sample containing 1.25 mol of nano-Al<sub>2</sub>O<sub>3</sub>. All results are correlated and discussed.

© 2013 Elsevier B.V. All rights reserved.

## 1. Introduction

Over the last decades, many polymer electrolytes based on metal salts dissolved in polyethers, particularly polyethylene oxide (PEO), have widely been investigated because of their potential applications in high-performance polymer batteries. Such electrolytes have mainly been confined to alkali metal salt systems, with particular attention being focused on lithium [1]. Solid polymer electrolytes for lithium batteries have many advantages over their counterpart liquid electrolytes, such as processing flexibility, but their conductivity at room temperature is usually too low to be applicable. This can be overcome by the ionic conductivity improvement of these electrolytes using fillers. At least, there are two types of fillers to improve the ionic conductivity of PEO-based polymer electrolytes. One is small organic molecules, such as ethylene carbonate (EC) and propylene carbonate (PC) [2], which can enhance the polymer electrolyte conductivity to a moderate value. At the same time, the disadvantage of the organic molecule fillers is that they are more expensive compared to inorganic ones.

The other one is that the dry inorganic compounds as ceramic powders, can enhance not only the conductivity but also the stability of the polymer in the meantime [3]. In this paper, nano-Al<sub>2</sub>O<sub>3</sub> with an average particle size of 42 nm was synthesized using pyrolysis method and then used to prepare polymer nano-composite electrolytes (Al<sub>2</sub>O<sub>3</sub>)<sub>x</sub>(PEO)<sub>12.5-x</sub>(LiClO<sub>4</sub>) (*x* = in the range of 0–1.25) as a ceramic filler. The results showed an ionic conductivity

of the polymer electrolyte with the highest value of  $8.3 \times 10^{-5}$  ohm<sup>-1</sup> cm<sup>-1</sup>, at room temperature, for the sample containing 1.25 mol Al<sub>2</sub>O<sub>3</sub>.

## 2. Experimental

Materials: pure reagent materials of Aluminium nitrate (Merk), Triethanol amine (Fluka), Sucrose (Fluka), PEO (with an average molecular weight of  $8 \times 10^6$ , Segma–Aldrich) and LiClO<sub>4</sub> (Segma–Aldrich) were used as starting materials to prepare nano-filler and polymer nano-composite electrolytes.

### 2.1. Preparation of nano-Al<sub>2</sub>O<sub>3</sub> filler

Nano-Al<sub>2</sub>O<sub>3</sub> was prepared using a method reported by Pramanik [4]. According to this method, a required amount of aluminium nitrate [Al(NO<sub>3</sub>)<sub>3</sub>·9H<sub>2</sub>O] was mixed with an equal amount of distilled water to get a pasty like mass. This material was then added to triethanol amine (TEA) to make a viscous solution. At the beginning, TEA formed a precipitate of aluminium hydroxide which dissolved and a clear solution was obtained by heating at about 150 °C. A sucrose solution was added to this resulting solution at a ratio of metal to sucrose is 1:4 and a few drops of HNO<sub>3</sub> were added to maintain the pH at 3–4. The clear solutions of TEA complexed metal nitrates with sucrose were evaporated on a hot plate at 180 °C. The continuous heating of these solutions causes foaming and puffing. During evaporation, the nitrate ions provide an in situ oxidizing environment for TEA which partially converts the hydroxyl groups of TEA and sucrose to carboxylic acids. When complete hydration occurs, the nitrates themselves are decomposed with the evolution of brown fumes of nitrogen dioxide leaving behind voluminous, organic based, black fluffy powders. The precursor powders, after grinding, were calcined at 1150 °C for 1 h to get nano-alpha Al<sub>2</sub>O<sub>3</sub>.

### 2.2. Preparation of polymer nano-composite electrolytes

The composite samples were synthesized by the conventional solution cast technique. PEO and LiClO<sub>4</sub> were dissolved in acetonitrile and magnetically stirred to get a homogeneous solution. An appropriate weight of nano-aluminium oxide

\* Corresponding author. Tel.: +20 1203532343.

E-mail address: [emad\\_masoud1981@yahoo.com](mailto:emad_masoud1981@yahoo.com) (E.M. Masoud).

was then added to the solution and stirred for 6 h to get a white viscous solution with high homogeneity. After that, the viscous solution was poured on pater dish and left to dry at room temperature for 2 days to allow the slow solvent evaporation. The prepared films with different filler concentrations were then dried under vacuum for 10 h and kept in a desiccator.

### 2.3. Characterization of samples

X-ray diffraction were performed on the investigated samples using a Philips X-ray diffractometer (Model PW 1710) with Cu K $\alpha$  radiation ( $\lambda = 1.54 \text{ \AA}$ ) in the range of  $2\theta = 4\text{--}60^\circ$ . Thermal analysis was performed for investigated samples in air atmosphere and at a temperature range of 298–353 K using differential scanning calorimetry technique (DSC) (Shimadzu DSC-60H). FT-IR spectra of the samples were recorded in the range of 400–4000  $\text{cm}^{-1}$  using KBr pellet technique on IR-Brucker, Vector 22, Germany. The electrical measurements were carried out on the samples in the form of films. The two parallel surfaces of the films were coated with silver paste to ensure good electrical contact. Each sample investigated was located in a sample holder inside a cryostat with a temperature controller of  $\pm 0.01^\circ\text{C}$  accuracy. The electrical conductivity was measured at a constant voltage (1 V) by using programmable automatic LCR bridge (model RM 6306 phillips bridge).

## 3. Results and discussion

The XRD pattern of  $\text{Al}_2\text{O}_3$  is shown in Fig. 1. It shows typical peak patterns characterized for  $\text{Al}_2\text{O}_3$ . XRD line broadening was used to estimate the grain size of the powder according to Scherrer formula [5]

$$D = 0.9\lambda/\beta \cos \theta \quad (1)$$

where  $D$  is the average diameter of the grains,  $\lambda$  is the wavelength of X-ray,  $\theta$  is the Bragg angle and  $\beta$  is the full width half maximum in radians calculated using Gaussian fitting. The results showed an average crystalline size of about 42 nm. XRD of pure PEO and investigated composites are also shown in Fig. 1. The

XRD of PEO polymer showed a crystalline behavior due to appearance of characteristic diffraction peaks in the range of  $2\theta = 19\text{--}23^\circ$  [6]. Whereas, the XRD of the composites containing  $\text{LiClO}_4$  and nano- $\text{Al}_2\text{O}_3$  showed a remarkable reduction in the intensity of XRD peaks of pure PEO, specially for the sample containing 1.25 mol  $\text{Al}_2\text{O}_3$ , which showed a complete amorphous nature. This can be attributed to a destruction effect of the filler on the ordered arrangement of the polymer side chains, and also as a result of enhancement of the amorphous phase.

DSC thermograms of pure PEO and  $(\text{Al}_2\text{O}_3)_x(\text{PEO})_{12.5-x}(\text{LiClO}_4)$ , ( $x = 0, 0.25, 0.75, 1$ , and 1.25 mol) were displayed in Fig. 2. The relative percentage of crystallinity ( $X_c$ ) has been calculated by taking into account 100% crystallinity for pure PEO [6] and using the equation

$$X_c = \Delta H_c/\Delta H_p \quad (2)$$

where  $\Delta H_p$  equals to 203 J/g which is the heat enthalpy of 100% crystalline PEO [6], and  $\Delta H_c$  is the heat enthalpy of composites. The calculated relative crystallinity ( $X_c$ ) and the data obtained from DSC thermograms are summarized in Table 1. From which, it can be seen that the melting temperature ( $T_m$ ) of the crystalline PEO phase decreases with increasing the amount of  $\text{Al}_2\text{O}_3$ . This refers to increase the flexibility of the composite samples with increasing the amount of  $\text{Al}_2\text{O}_3$  in the PEO matrix.

The FT-IR spectra of  $\text{Al}_2\text{O}_3$ , PEO,  $\text{LiClO}_4$  and  $(\text{Al}_2\text{O}_3)_x(\text{PEO})_{12.5-x}(\text{LiClO}_4)$ , ( $x = 0, 0.25, 0.75, 1$ , and 1.25 mol) are shown in Fig. 3. The spectra of the composite systems display some spectral features similar to those of pure PEO. However, the incorporation of both  $\text{LiClO}_4$  and nano- $\text{Al}_2\text{O}_3$  particles causes shifts of some PEO bands. At a frequency range of 1050–1160  $\text{cm}^{-1}$ , significant changes were observed in the width and intensity of the

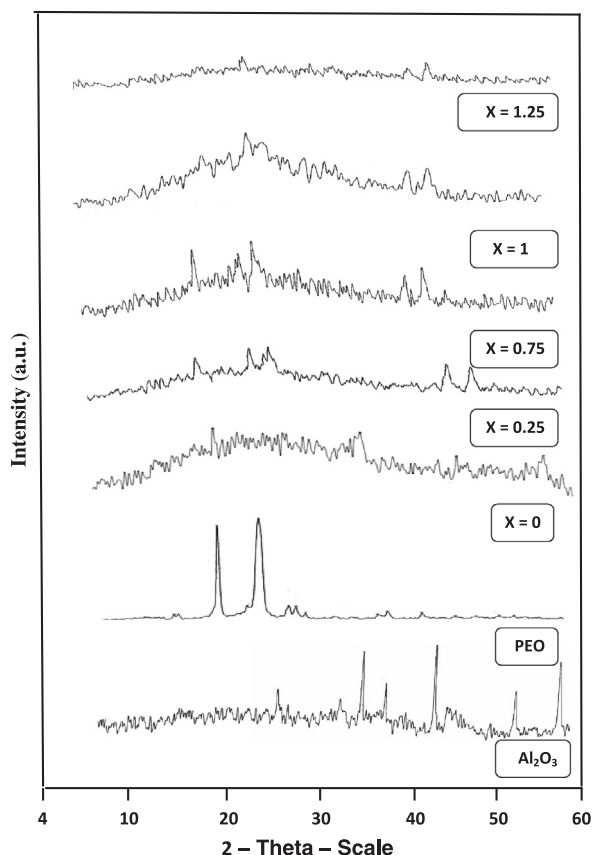


Fig. 1. XRD Patterns of  $\text{Al}_2\text{O}_3$ , pure PEO and  $(\text{Al}_2\text{O}_3)_x(\text{PEO})_{12.5-x}(\text{LiClO}_4)$ , ( $x = 0, 0.25, 0.75, 1$  and 1.25 mol).

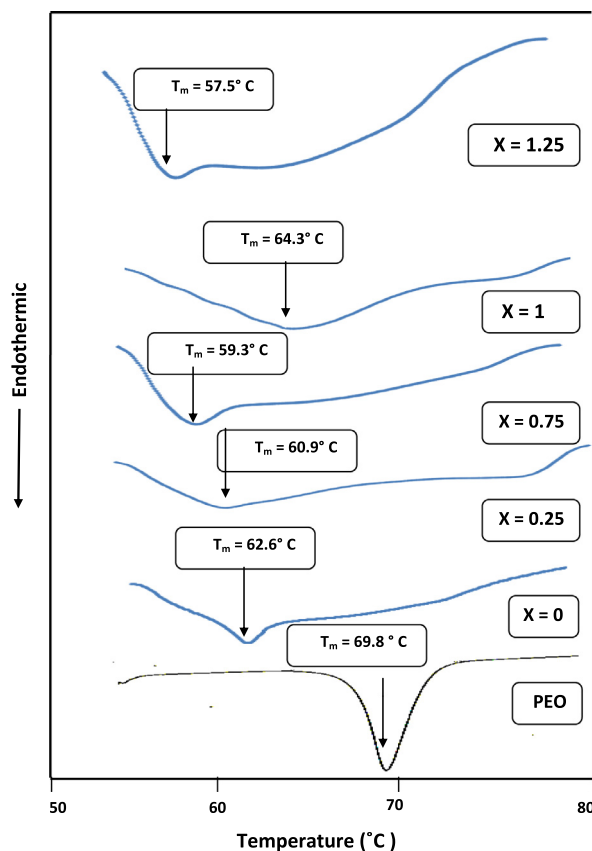
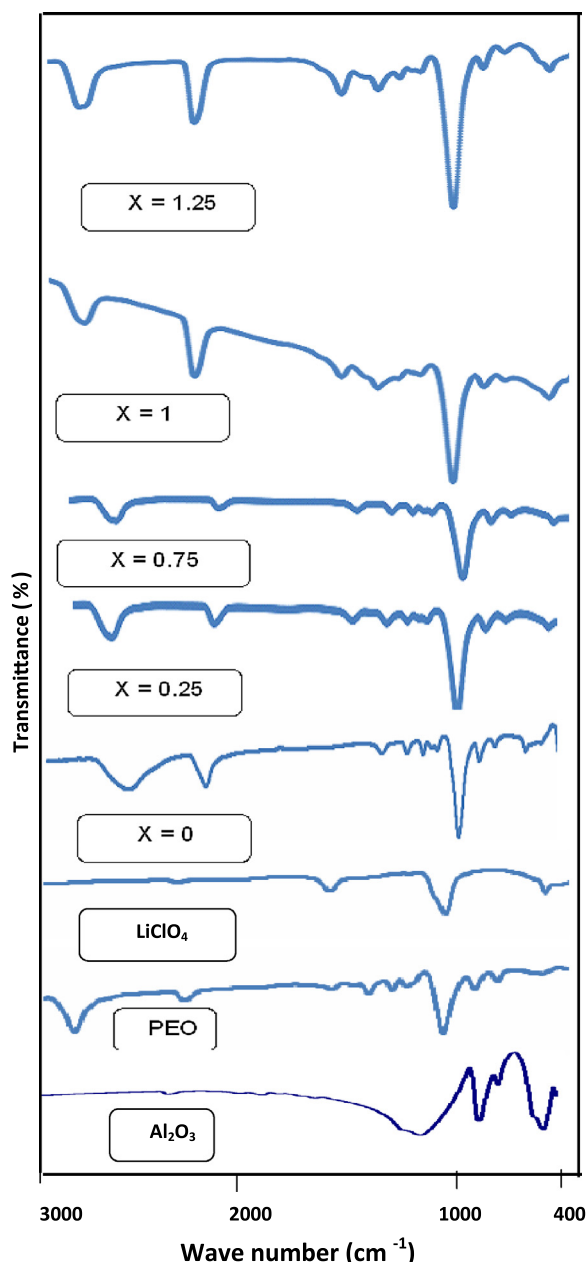


Fig. 2. DSC curves of pure PEO and  $(\text{Al}_2\text{O}_3)_x(\text{PEO})_{12.5-x}(\text{LiClO}_4)$ , ( $x = 0, 0.25, 0.75, 1$  and 1.25 mol).

**Table 1**  
Melting temperatures ( $T_m$ ), melting enthalpy ( $\Delta H_m$ ) and relative crystallinity ( $X_c$ ) for  $(Al_2O_3)_x(PEO)_{12.5-x}(LiClO_4)$ .

(X), (mol)	$T_m$ (°C)	$H_m$ (J/g)	$X_c$ (%)
Pure PEO	69.8	139.1	68.5
0	62.6	52.3	25.8
0.25	60.9	190	93.6
0.75	59.3	88	43.4
1	64.3	170.7	84.1
1.25	57.5	50.3	24.8



**Fig. 3.** FT-IR patterns of  $Al_2O_3$ , PEO,  $LiClO_4$  and  $((Al_2O_3)_x(PEO)_{12.5-x}(LiClO_4))$ , ( $x = 0, 0.25, 0.75, 1$  and  $1.25$  mol).

vibrational bands of PEO due to the addition of  $LiClO_4$  salt and nano- $Al_2O_3$  filler. These changes were attributed to the effect of both  $LiClO_4$  and nano- $Al_2O_3$  on C–O–C symmetric vibrational modes. Metal oxygen stretching frequency of  $463\text{ cm}^{-1}$  in pure  $Al_2O_3$  is shifted to  $587\text{ cm}^{-1}$  in the composite indicating the Van-der-Waals interaction between  $Al_2O_3$  and PEO polymer. Generally,

the changes occurring in IR spectra confirm the interaction process in the polymer nano-composite electrolytes samples with each of  $Al^{3+}$  and  $Li^+$  ions. This interaction may be associated with the interaction of  $Al^{3+}$  ion and oxygen atom in PEO macromolecule. Also, the interaction may weaken the bond strengths of C–O–C in PEO macromolecule.

### 3.1. DC-electrical conductivity

The temperature dependence of electrical conductivity (DC) of  $(Al_2O_3)_x(PEO)_{12.5-x}(LiClO_4)$ , ( $x = 0, 0.25, 0.75, 1$ , and  $1.25$  mol) is investigated in a temperature range of 293–323 K and illustrated in Fig. 4. The overall feature of the plots is almost similar for pure PEO and all investigated composites. The conductivity data are summarized and given in Table 2. Generally, it can be seen that the addition of nano- $Al_2O_3$  in the PEO– $LiClO_4$  matrix causes a high enhancement in the conductivity of the composite electrolyte. Electrical conductivity reached a value higher 100 times than that of the polymer electrolyte system PEO– $LiClO_4$ , Table 2. The increase in conductivity may be attributed to an increase occurring in the flexibility of the composite by introducing  $Al_2O_3$  into PEO matrix, due to the high interface area between the matrix and the dispersed nano- $Al_2O_3$  particles [7,8]. Moreover, the increase in amorphous phase within the PEO-matrix due to the addition of nano- $Al_2O_3$  causes an enhancement in the segmental motion of the polymer chains and hence increases the conductivity.

The small particle of  $Al_2O_3$  in our samples (42 nm) was more efficient than that of 300 nm reported before by Qian [9] for the same system of PEO– $LiClO_4$ , where it showed an ionic conductivity value equals  $5.29 \times 10^{-6}\text{ ohm}^{-1}\text{ cm}^{-1}$  at room temperature. This shows that the small particle size of filler plays an important role in enhancing the conductivity of the system.

Fig. 5 shows a nonlinear increase in conductivity of the composite with increasing the concentration of nano- $Al_2O_3$  filler. This increase is possibly due to the dissociation of salt ion aggregates into the free ions with the addition of nano-sized  $Al_2O_3$  particles. The conductivity results, Table 2, showed the highest conductivity value for the sample containing 1.25 mol  $Al_2O_3$  because its high amorphous structure (XRD) enhancing the transport of ionic charge carriers, as will be seen later.

The observed increase of conductivity with temperature, Fig. 4, can be attributed to the viscosity decrease and hence, an improvement of the sample flexibility chain [10]. The conductivity data present in Table 2 shows a higher activation energy value (0.46 eV) for the free  $Al_2O_3$  filler sample than that of the sample containing 1.25 mol  $Al_2O_3$  filler (0.19 eV). This low value of activation energy can be attributed to the amorphous nature facilitating the  $Li^+$  ion motion in the polymer network [11], as shown in the results of impedance. The electrical devices that work over a wide temperature range should have uniform conductivity, thus, materials with low activation energy is a good electrical system [12]. Therefore, according to the above results the composite system containing 1.25 mol nano- $Al_2O_3$  was chosen to be more studied using AC-conductivity, dielectric behavior, and impedance character.

### 3.2. Impedance spectroscopy analysis

Impedance plots ( $Z'$  vs.  $Z''$ ) in the complex plan for  $(Al_2O_3)_{1.25}(PEO)_{11.25}(LiClO_4)$  at different temperatures showed a similar behavior. A typical plot is shown in Fig. 6, which demonstrates a depressed semicircular portion followed by a spike. This spike refers to an ionic conductivity and is characteristic of a blocking double layer capacitance whose magnitude can be estimated from any position on the spike using the equation.  $Z'' = 1/2\pi fC_{dl}$ , where  $f$  is the frequency and  $C_{dl}$  is the capacitance at the frequency

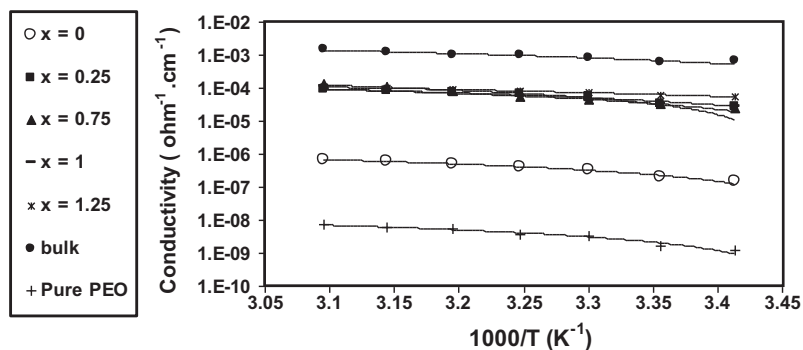


Fig. 4. Temperature dependence of both DC-conductivity for pure PEO and composite samples with different  $x$  values and bulk conductivity at  $x = 1.25$  mol.

Table 2

DC and bulk conductivity ( $\sigma_{dc}$ ,  $\sigma_b$ ) data for  $(Al_2O_3)_x(PEO)_{12.5-x}(LiClO_4)$  at room temperature (293 K).

(X), (mol)	$E_a$ (eV)	$\sigma_{dc}$ ( $ohm^{-1} cm^{-1}$ )	$\sigma_b$ ( $ohm^{-1} cm^{-1}$ )	$E_a$ (eV)
Pure PEO	0.40	$1.25 \times 10^{-9}$	$7.00 \times 10^{-7}$	0.33
0	0.46	$1.55 \times 10^{-7}$	$1.60 \times 10^{-4}$	0.55
0.25	0.33	$4.30 \times 10^{-5}$	$2.50 \times 10^{-4}$	0.34
0.75	0.48	$3.80 \times 10^{-5}$	$7.08 \times 10^{-5}$	0.82
1	0.36	$4.50 \times 10^{-5}$	$2.75 \times 10^{-4}$	0.45
1.25	0.19	$8.30 \times 10^{-5}$	$6.45 \times 10^{-4}$	0.24

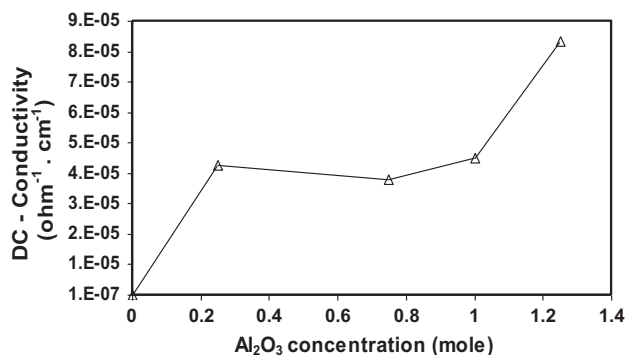


Fig. 5.  $Al_2O_3$  concentration dependence of DC-conductivity ( $\sigma_{dc}$ ) for  $(Al_2O_3)_x(PEO)_{12.5-x}(LiClO_4)$ , ( $X = 0, 0.25, 0.75, 1, 1.25$  mol) at room temperature (293 K).

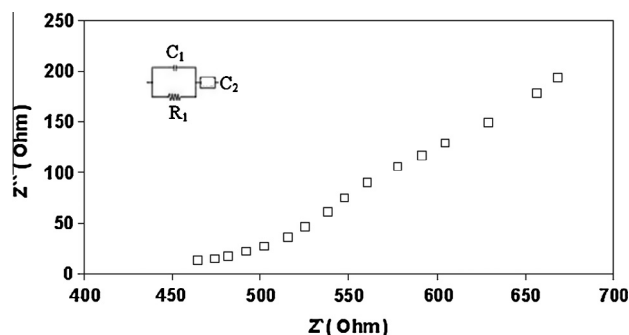


Fig. 6. Plot of  $Z''$  vs.  $Z'$  for  $(Al_2O_3)_{1.25}(PEO)_{11.25}(LiClO_4)$ , at room temperature (293 K).

The ionic conductivity of the solid polymer nano-composite electrolyte  $(Al_2O_3)_{1.25}(PEO)_{11.25}(LiClO_4)$  was derived from the ac impedance analysis. The high depression of semicircular portion at high frequencies, in complex impedance, is a result of the ionic conductivity increase with frequency increasing [7]. The equivalent circuit of the polymer nano-composite electrolyte system is determined from the complex impedance spectrum and given in

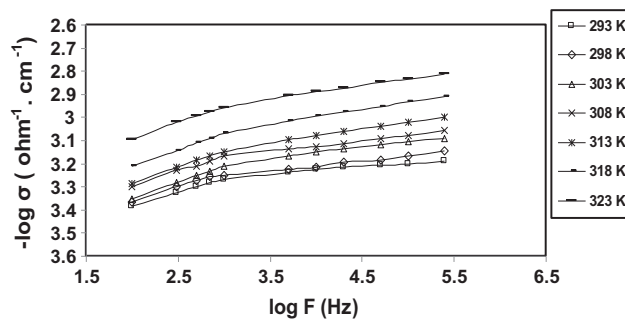


Fig. 7. Variation of AC-electrical conductivity with frequency at different temperatures for  $(Al_2O_3)_{1.25}(PEO)_{11.25}(LiClO_4)$ .

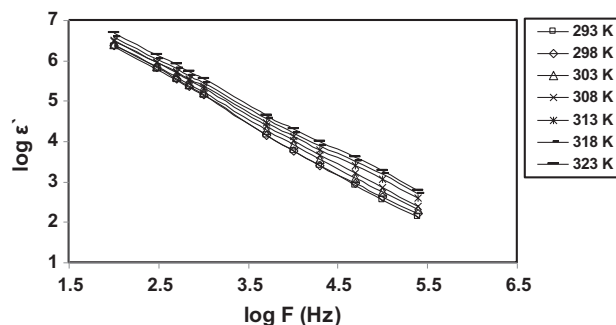


Fig. 8a. Variation of dielectric constant with frequency at different temperatures for  $(Al_2O_3)_{1.25}(PEO)_{11.25}(LiClO_4)$ .

Fig. 6, where  $R_1$  is the bulk resistance of the electrolyte,  $C_1$  is the bulk capacity of the electrolyte and  $C_2$  is a capacity of bulk electrode–electrolyte interface. The bulk ionic conductivity of  $6.45 \times 10^{-4} ohm^{-1} cm^{-1}$  at room temperature was calculated using the equation  $\sigma_b = L/R_b A$ , where  $L$  is the thickness of the polymer nano-composite electrolyte film and  $A$  is its surface area. The resistance of the electrolyte ( $R_b$ ) was determined from the intercept of the impedance spectrum on the  $Z'$  real axis. The temperature dependence of the bulk conductivity showed a linear behavior, Fig. 4, as that reported by DC-conductivity. The bulk conductivity data are also reported in Table 2. The difference between DC and impedance data is attributed to the grain boundaries present between the particles.

### 3.3. AC-conductivity

In order to give information on polarization type present in  $(Al_2O_3)_{1.25}(PEO)_{11.25}(LiClO_4)$  sample, the ac-electrical conductivity

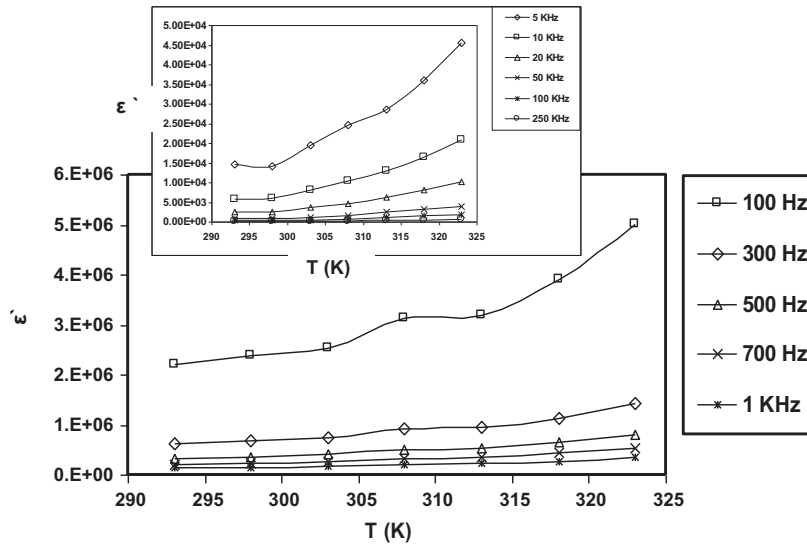


Fig. 8b. Variation of dielectric constant with temperature at different frequencies for  $(Al_2O_3)_{1.25}(PEO)_{11.25}(LiClO_4)$ .

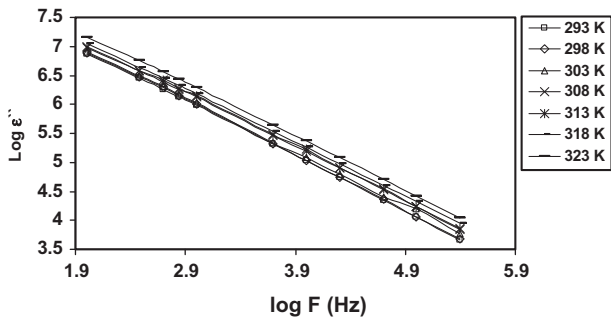


Fig. 9a. Variation of dielectric loss with frequency at different temperatures for  $(Al_2O_3)_{1.25}(PEO)_{11.25}(LiClO_4)$ .

( $\sigma_{ac}$ ) at temperatures between 293 and 323 K and a frequency range of  $10^2$ – $10^5$  Hz was studied, Fig. 7. It can be seen that the conductivity increases with each of frequency and temperature. The

frequency dependence of conductivity is attributed to the change occurring in mobility of charge carriers. The increase in  $\sigma_{ac}$  with temperature can be explained on the basis that raising the temperature causes more structure relaxation and releasing more of  $Li^+$  ions attached oxygen of PEO to become more mobilized. This may be also due to increasing the drift mobility and hopping frequency of charge carriers.

### 3.4. Dielectric permittivity and loss studies

The frequency dependence of dielectric constant  $\epsilon'$  at different temperatures for  $(Al_2O_3)_{1.25}(PEO)_{11.25}(LiClO_4)$  sample is shown in Fig. 8a. It can be seen that  $\epsilon'$  decreases as frequency increases. This decrease is relatively sharp at lower frequencies and slow at higher ones. The decrease in dielectric permittivity with frequency increasing can be associated to the inability of dipoles to rotate rapidly leading to a lag between frequency of oscillating dipole and that of applied field [13]. The dielectric permittivity obtained in our system ( $\epsilon' = 2.21 \times 10^6$ , at room temperature) is higher than

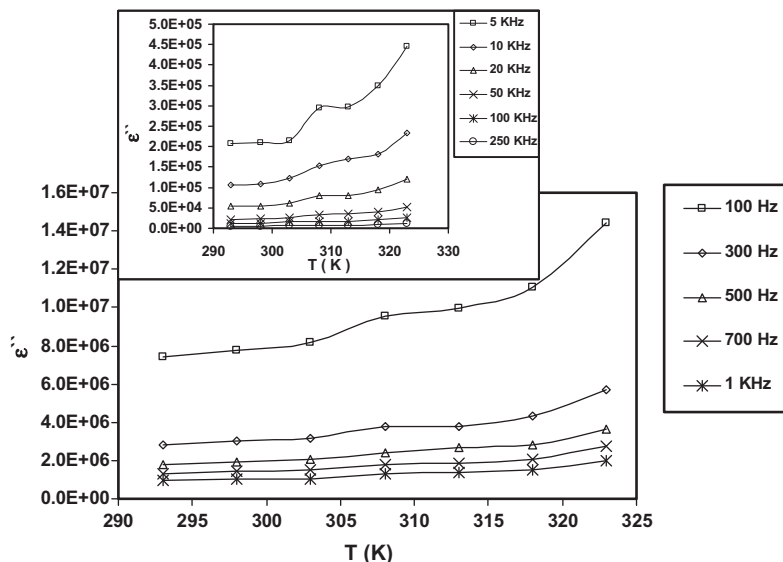


Fig. 9b. Variation of dielectric loss with temperature at different frequencies for  $(Al_2O_3)_{1.25}(PEO)_{11.25}(LiClO_4)$ .

that of other polymer electrolyte systems ( $\epsilon'$  lie in the range of  $9.8 \times 10^3$ – $4.4 \times 10^5$ , at room temperature). Such high dielectric constant values can be attributed to the high ionic conductivity on account of the presence of nano-particles of aluminium oxide and its good distribution within the matrix of poly ethylene oxide and also due to the good interactions between the Lewis acidic sites on the surface of those particles and the ions of lithium perchlorate [14]. When the temperature is raised, dielectric constant also enhances due to the facilitation in orientation of dipoles within the matrix of PEO [15].

The temperature dependence of dielectric constant at different frequencies is shown in Fig. 8b. The variation of dielectric constant with temperature can be divided into two ranges, in the low temperatures range (from 293 to 298 K), the change of dielectric constant is weakly dependent on the temperature but in the high ones range (from 298 to 323 K), the dielectric constant is strongly dependent on it. The increase of dielectric constant with temperature is generally attributed to two mechanisms. The first is to the viscosity decrease of the polymer nano-composite electrolyte [16] and the second is to the dissolving of any small concentration of crystalline and semi-crystalline phases into the amorphous phase [13]. This is in turn influences the polymer dynamics and thus the dielectric behavior. The presence of the two ranges in Fig. 8b may be attributed to the effect of the two mechanisms. Whereas at low temperature range, the viscosity is low and crystalline phases are present, thus the dielectric behavior is weakly dependent on the temperature; while at high one range, the opposite trend is predominate.

Fig. 9a and 9b) shows the variation of dielectric loss  $\epsilon''$  with frequency and temperature for  $(\text{Al}_2\text{O}_3)_{1.25}(\text{PEO})_{11.25}(\text{LiClO}_4)$  sample. The observed behaviors are similar to those of dielectric constant. Where the dielectric loss decreased with increasing the frequency due to high periodic reversal of the field at the interface, the contribution of charge carriers (ions) towards the dielectric loss decreases with frequency increasing and this decreasing can be attributed to the reduction of the ions diffusion in the polymer matrix with frequency increase. The increase of dielectric loss with temperature increasing can be also attributed to the dipoles relaxation in cooperation with the resulting drop in the relaxation time.

#### 4. Conclusions

Nano-sized  $\text{Al}_2\text{O}_3$  filler with an average particle size of 42 nm was prepared by pyrolysis method.  $(\text{Al}_2\text{O}_3)_x(\text{PEO})_{12.5-x}(\text{LiClO}_4)$

composite electrolytes containing nano-sized  $\text{Al}_2\text{O}_3$  particles with concentration of  $x = 0.25, 0.75, 1$  and  $1.25$  mol were synthesized. The samples were characterized using DSC, X-ray diffraction and Infra-red spectra. The shifts, broadening and reduction in the intensity of the IR-bands confirm the dissolution of the metal salt in the polymer matrix. The DSC analysis revealed to a change in the crystallinity and melting points of the composite samples with the different filler concentrations. All composite samples showed an ionic conductivity, in which the addition of nano- $\text{Al}_2\text{O}_3$  particles enhances the ionic conductivity of the based polymer electrolyte by hundred times at room temperature. The sample containing 1.25 mol of nano- $\text{Al}_2\text{O}_3$  showed the highest conductivity value ( $8.3 \times 10^{-5} \text{ ohm}^{-1} \text{ cm}^{-1}$ ) at room temperature for all samples. The electrical properties of investigated sample showed dielectric permittivity and loss values of  $2.21 \times 10^6$  and  $7.42 \times 10^6$  at room temperature, respectively. The high values of DC-conductivity, dielectric permittivity and dielectric loss at room temperature for the investigated composite electrolyte lead to make the sample as a promising material for lithium battery as an application in the solid state electrochemical devices.

#### References

- [1] M.A.K.L. Dissanayake, L.R.A.K. Bandara, L.H. Karaliyadda, P.A.R.D. Jayathilaka, R.S.P. Bokalawala, *Solid State Ionics* 177 (2006) 343.
- [2] A.G. Bishop, D.R. Macfarlane, D. McNaughton, M. Forsyth, *J. Phys. Chem.* 100 (1996) 2237.
- [3] E. Quartarone, P. Mustarelli, A. Magistris, *Solid State Ionics* 110 (1998).
- [4] A. Janbey, R.K. Pati, S. Tahir, P. Pramanik, *J. Eur. Ceram. Soc.* 21 (2001) 2285.
- [5] H.P. Klug, L.E. Alexander, *X-ray Diffraction Procedures for Polycrystalline and amorphous Materials*, Wiley, New York, 1970.
- [6] B. Wunderlich, *Macromolecular Physics*, Academic press, New York, 1980. vol. 3, pp. 7.
- [7] L. fan, Z. Dang, G. Wei, C. Nan, M. Li, *Mater. Sci. Eng. B* 99 (2003) 340.
- [8] J. Maier, *Solid State Ionics* 75 (1995) 139.
- [9] X. Qian, N. Gu, Z. Cheng, X. Yang, E. Wang, S. Dong, *Electrochimica Acta* 46 (2001) 1829.
- [10] K. Tsunemi, H. Ohno, E. Tsuchida, *Electrochimica Acta* 28 (6) (1983) 833.
- [11] R. Baskaran, S. Selvasekarapandian, N. Kuwata, J. Kawamura, T. Hattori, *J. Phys. Chem. Solids* 68 (2007) 407.
- [12] J.M.G. Cowie, G.H. Spence, *Solid State Ionics* 109 (1998) 139.
- [13] A. Awadhia, S.K. Patel, S.L. Agrawal, *Prog* 52 (2006) 61.
- [14] H.M. Xiong, X. Zhao, J.S. Chen, *Phys. Chem. B* 105 (2001) 10169.
- [15] C.A. Finch, *Polyvinyl Alcohol: Properties and Applications*, John Wiley & Sons Ltd., London, 1973.
- [16] K.P. Singh, P.N. Gupta, R.P. Singh, *J. Polym. Mater.* 9 (1992) 131.